

# 1        **Three-dimensional X-ray imaging and analysis of fungi on and in wood**

2

3        **Running head:** X-ray imaging of fungi

4

5        Jan Van den Bulcke<sup>1</sup>, Matthieu Boone<sup>2</sup>, Joris Van Acker<sup>1</sup>, Luc Van Hoorebeke<sup>2</sup>6        <sup>1</sup>Laboratory of Wood Technology, Faculty of Bioscience Engineering, Ghent University,

7        Coupure Links 653, 9000 Gent, Belgium

8        <sup>2</sup>Department for Subatomic and Radiation Physics, Faculty of Sciences, Ghent University,

9        Proeftuinstraat 86, 9000 Gent, Belgium

10

11        \*e-mail: [Jan.VandenBulcke@UGent.be](mailto:Jan.VandenBulcke@UGent.be)

12        postal address:        Ghent University

13                                Laboratory of Wood Technology

14                                Coupure links 653

15                                9000 Ghent

16                                Belgium

17        **tel:** + 0032 (0)9 264 61 2418        **fax:** + 0032 (0)9 264 62 33

19

20        Cite as:

21        Van den Bulcke, J., Boone, M., Van Acker, J., Van Hoorebeke, L. (2009b). Three-

22        dimensional X-ray imaging and analysis of fungi on and in wood. *Microscopy and*23        *Microanalysis* 15(5): 395-402. DOI: 10.1017/S1431927609990419

24 **Abstract**

25

26 As wood is prone to fungal degradation, fundamental research is necessary to increase our  
27 knowledge aiming at product improvement. Several imaging modalities are capable of  
28 visualizing fungi, but the X-ray equipment presented in this paper can envisage fungal  
29 mycelium in wood non-destructively in three dimensions with sub-micron resolution. Four  
30 types of wood subjected to the action of the white rot fungus *Coriolus versicolor* (Linnaeus)  
31 Quélet (CTB 863 A) were scanned using an X-ray based approach. Comparison of wood  
32 volumes before and after fungal exposure, segmented manually or semi-automatically,  
33 showed the presence of the fungal mass on and in the wood samples and therefore  
34 demonstrated the usefulness of computed X-ray tomography for mycological and wood  
35 research. Further improvements to the experimental set-up are necessary in order to resolve  
36 individual hyphae and enhance segmentation.

37

38

## 39 **1. Introduction**

40

41 As a sustainable material, wood has a considerable advantage compared to other building  
42 materials such as concrete and steel. Its susceptibility to attack and degradation by  
43 microorganisms is considered a disadvantage. Fungi cause the most serious kind of  
44 microbiological deterioration, leading to rapid structural failure (Green & Highley, 1997).

45 Wood biodeterioration also affects the artistic and cultural value of historical buildings and  
46 monuments (Gutiérrez et al., 1995). Apart from its detrimental action, fungal degradation of  
47 lignocellulose is also probably the most important process for recycling carbon in nature  
48 (Eriksson et al., 1990).

49 Traditionally, wood is protected using biocidal treatment by impregnation or superficial  
50 application. Increasing environmental concerns during the last decade have initiated a shift to  
51 less toxic methods for the preservation of wood and an increased interest in protection by  
52 design. This could be facilitated if the process of degradation was better understood.  
53 Furthermore, the lack of accurate and rapid non-destructive methods to detect and quantify  
54 wood decay is one of the factors that hinders service life prediction of wooden constructions  
55 and commodities (Råberg et al., 2007).

56 In general, three types of wood rot can be distinguished: soft rot, brown rot and white rot.  
57 Especially the white rot basidiomycetes are known to be active wood degraders since they  
58 secrete a wide range of hydrolytic and oxidative enzymes (Nicole et al., 1993) and as such are  
59 able to degrade lignin efficiently (Mansur et al., 2003). Like most other fungi, they are able to  
60 persist in dynamic, heterogeneous environments because of the capacity to take locally  
61 immobilized internal resources and remobilize these into a form capable of being reused  
62 locally or directed to new internal sinks through their hyphal network (Falconer et al., 2005).  
63 These hyphae, the basic units of the mycelium, are the core of their successful invading

64 capabilities. Part of the research concerning wood damaging fungi involves localization by  
65 visualizing the entire network as well as their basic units, which is difficult due to their small  
66 dimensions. Apart from conventional light microscopy of stained wood sections, many other  
67 techniques enable researchers imaging fungi. Hickey et al. (2005) have given a review of live-  
68 cell imaging of filamentous fungi using vital fluorescent dyes and confocal microscopy.  
69 Dickson & Kolesik (1999) also used confocal microscopy for the visualisation of mycorrhizal  
70 fungal structures and quantification of their surface area and volume. Muller et al. (2001,  
71 2002) employed magnetic resonance imaging for the detection of incipient fungal attack in  
72 wood. Other imaging modalities are cryo-FE-SEM and TEM immuno-techniques (Daniel et  
73 al., 2004). Especially low temperature SEM is a valuable tool (Refshauge et al., 2006) to  
74 examine samples with minimum disruption to structural integrity by rapidly freezing the  
75 specimen to temperatures below -130°C in which state the specimen is considered to be in a  
76 fully frozen hydrated condition (Beckett & Read 1986; Abu Ali et al., 1999). At last, X-ray  
77 analysis is a promising technique for mycological research. Illman and Dowd (1999)  
78 successfully used synchrotron-based X-ray microtomography to characterize wood degraded  
79 by decay fungi. Macchioni et al. (2007) explored X-ray microdensitometry for measuring  
80 fungal wood decay and Van den Bulcke et al. (2008) explored X-ray sub-micron tomography  
81 for examination of coated wood disfigured by blue stain fungi. Advantages are the non-  
82 destructiveness, penetrative power, acquisition speed and three-dimensional imaging of the  
83 substrate giving a large field of view on the internal structure at sub-micron resolution.  
84 To assess the usefulness of X-ray tomography for wood decay research, four types of wood  
85 were inoculated with the white rot fungus *Coriolus versicolor* (Linnaeus) Quélet (CTB 863  
86 A) and scanned with a state-of-the-art X-ray instrument. Samples were examined before and  
87 after exposure to the fungal culture and compared using manual segmentation. An attempt to  
88 use differential imaging is presented as well.

89

## 90 **2. Materials and Methods**

91

92 Wood from the following tree species was used in this study: Scots pine (*Pinus silvestris* -  
93 sapwood), beech (*Fagus sylvatica*), movingui (*Disthemonanthus benthamianus*) and afzelia  
94 (*Afzelia bipindensis*), representing hardwood and softwood as well as temperate and tropical  
95 wood types. Pine sapwood and beech are often used in European standards related to  
96 Basidiomycota testing whereas movingui and afzelia are durable tropical species on the  
97 market. Samples were prepared by slicing a thin wood section of a larger block and  
98 subdividing it with a microtome into needle-shaped specimens. The tip of the wood sample,  
99 measuring approximately one mm<sup>3</sup>, was scanned before exposure to fungi, using the X-ray  
100 equipment built at the Centre for X-ray Tomography at Ghent University (UGCT -  
101 <http://www.ugct.ugent.be>). This is a state-of-the-art scanner (Masschaele et al., 2007), highly  
102 flexible, with in-house developed software for scanner control, sample reconstruction,  
103 analysis and visualization. The X-ray source, a Feinfocus nano-focus tube, has a focal spot  
104 size < 1 µm. All samples were scanned at an average tube voltage of 50 kV, a current of 40  
105 µA and an exposure time of 1500 ms per image. A rotation step size of 0.36° was used.  
106 Reconstruction took 20 min with Octopus, a server/client tomography reconstruction package  
107 for parallel and cone beam geometry (Vlassenbroeck et al., 2007). With the described set-up,  
108 sub-micron resolution can be reached, resulting in scans with voxels sizing approximately 0.7  
109 x 0.7 x 0.7 µm. The small voxel size gives a clear view of anatomical features as described in  
110 Van den Bulcke et al. (2008). After scanning the non-decayed specimen, needle-shaped  
111 samples were exposed to *Coriolus versicolor*. The fungus was cultured in several Petri dishes  
112 on a nutrient medium (20 g agar, 40 g malt extract in 1 L water) at 23°C for one week, after  
113 which wood samples were put on the fungus. Scans were acquired twice, once after 1 week

114 and once after 6 weeks with similar tuning of the equipment. Obviously, as samples were  
115 scanned in a non-sterile environment, contamination of the samples and of the culture upon  
116 replacement could not be excluded due to the presence of airborne fungal spores. This was not  
117 a major issue as the objective of the experiment was mainly to assess the use of X-ray  
118 tomography for fungal visualization. Furthermore, as samples were exposed to non-sterile  
119 conditions only after one week of incubation, the cultured fungus already grew on and in the  
120 sample and was most likely the dominant fungal species. The radiation dose during a standard  
121 scan was monitored by measuring the optical density of a radiochromic fluid with a FWT-200  
122 opti-chromic reader system and was found to be approximately 20 Gy.

123 Reconstructed images of the different samples before and after fungal attack were visualized  
124 with VGStudio MAX<sup>®</sup>, Matlab<sup>®</sup> and Drishti (Limaye, 2006). Fungal tissue was manually  
125 separated from noise and substrate. Green is used as an arbitrary assignment of colour to the  
126 specimen density where fungal hyphae are located in the reconstructed images. An attempt  
127 was made for differential imaging by subtracting two volumes using the Drop software  
128 (Glocker et al., 2007; Komodakis et al., 2007) for non-rigid body registration. Accurate  
129 registration required pre-processing including histogram equalization, affine volume rotation  
130 (Van den Bulcke et al., 2008), resolution correction and volume cropping as a first rough  
131 alignment.

132

### 133 **3. Results**

134

135 At first, the wood samples were scanned before exposure to white rot fungi (Fig. 1).

136

137 **Figure 1.**

138

139 The images so obtained clearly illustrate the possibilities of sub-micron CT-scanning and  
140 resemble classical SEM recordings (McMillin, 1977). As a resolution below one  $\mu\text{m}$  is  
141 reached, cell walls, pits and other small scale structures are discernable on the radial cross-  
142 sections that accompany the volumes in Fig. 1. The range of greyscale levels equals  $2^{16}$ .

143

### 144 **3.1 Fruiting bodies outside wood**

145

146 Scanning of the wood samples involved removal from the Petri dish and exposure to airborne  
147 fungi resulting in the contamination of both the beech and the pine sample. The large fungal  
148 fruiting bodies on beech, present a few weeks after the second scan, were used as a test case  
149 for scanning and visualization of fungi with ionizing radiation. The black globular structures  
150 at the outside were identified as an *Aspergillus* species and other unidentified moulds. Fig. 2a  
151 is an image of beech with *Coriolus versicolor* and *Aspergillus* growing on the wood while  
152 Fig. 2b is a pine sample covered with *Coriolus versicolor* and other unidentified mould fungi.  
153 Both images were taken with a standard camera in the visible wavelength domain. Fig. 2c and  
154 2d represent their X-ray counterparts.

155

156 **Figure 2.**

157

158 The fruiting bodies are visualised easily, most likely due to their size and melanin content. A  
159 covering network of hyphae, either *Coriolus versicolor* (most probably) or a contaminant is  
160 also visible, but individual hyphae are very small and fuse easily with noise. Although the  
161 hyphal mass is discernable, individual hyphae are difficult to distinguish and exhibit a low  
162 contrast and unconnected links. Still, these small hyphae are of interest, particularly to what  
163 extent they are able to penetrate in the wood.

164

### 165 **3.2 Time series scanning**

166

167 Time recordings of the four wood species, before and after one and six weeks of exposure to  
168 the fungal culture, are examined in Fig. 3. Preprocessing of the original volumes included  
169 noise removal by histogram clipping, resampling and recoding of the grey scale values.  
170 Volumes are translated and rotated equally to facilitate comparison. All volumes consist of  $2^{16}$   
171 grey levels with a resolution ranging from 1.9  $\mu\text{m}$  down to 0.6  $\mu\text{m}$ .

172

173 **Figure 3.**

174

175 Apparently, the beech sample was damaged during preparation as can be seen from the  
176 rugged top section. Other samples are more or less parallelepiped shaped. The hyphae wind  
177 around the substrates, obviously more pronounced after 6 weeks. Especially the beech and  
178 movingui sample illustrate the presence of a mycelial coat at the outer boundaries. When  
179 taking a closer look, individual hyphae are discernible albeit difficult and the network is not  
180 fully connected. The pine images do not satisfy the aim of hyphal tracking and growth  
181 monitoring, as hyphae are difficult to see in the wood itself. For afzelia, hyphal masses are  
182 more pronounced due to the heterogeneous anatomy of the substrate, especially in the vessel  
183 region, probably because hyphae tend to coalesce in voids such as lumens and deteriorated  
184 rays and this is perhaps the reason why a signal for fungal density is given in these areas.

185

### 186 **3.3 Segmentation of fungal hyphae**

187



188 The X-ray density of the fungal hyphae is rather low, between air and wood, and especially  
189 the isolated hyphae tend to fade into noise due to their small size and partial volume effects.  
190 Segmentation based on the histogram is therefore rather difficult yet will give an idea of the  
191 distribution of the fungal hyphae in the larger voids of the substrate. It is crucial to find the  
192 range of grey level values that enclose the fungal hyphae. Fig. 4 illustrates the result of  
193 manual classification of mycelium (green) for the four wood species.

194

195 **Figure 4.**

196

197 Green patches are present in all four samples, with explicit growth in large anatomical  
198 structures such as vessels. When looking more closely to the pinewood sample, it is  
199 remarkable that fungal penetration in depth in the wood is limited. When examining the  
200 bordered pits, degradation of the tori is visible, similar to what is shown in Schwarze (2007).  
201 Although fungal tissue is visualised with manual segmentation, the partial volume effect at  
202 the edge of wood can result in falsely detected fungus on this position. It is also subjective,  
203 incriminating quantitative and even precise qualitative analysis. To investigate the difference  
204 between samples in an objective way, differential imaging would be appropriate.

205

### 206 **3.4 Differential imaging**

207

208 Application of Drop software permitted image subtraction to reveal areas with differing  
209 density on a pre-processed subvolume of pine sapwood. These areas included fungal hyphae  
210 primarily, also apparently included degraded wood zones, and potentially other features with  
211 changed density. A 2D cross-section is shown with the original images (Fig. 5a and 5b) and  
212 their difference (Fig. 5c).

213

214 **Figure 5.**

215

216 Although fungal tissue is visible as well (bottom left hand corner), a considerable amount of  
217 incorrect transformation artefacts are masking most of them. The edges of the images seem  
218 difficult to register. Especially the inner parts are deformed correctly as only a faint print of  
219 the wood structure remains.

220

#### 221 **4. Discussion**

222

223 In the present study it is shown that fungi on and in wood can be imaged non-destructively  
224 using X-ray computed tomography with sub-micron resolution. It should be stressed that  
225 scanning at high resolution is non-trivial. Sub-micron scans for small samples require small  
226 spot sizes implying low fluxes and hitherto long scanning times. Deviations in the stability of  
227 the sample and of the X-ray spot by thermal effects of the X-ray tube should be overcome,  
228 just as inaccuracies in the positioning of the rotation motor and anomalies of the geometric  
229 accuracy of the detector. A motion compensation procedure is imperative (Vidal et al., 2005)  
230 in addition to filtering and normalisation. Results give evidence for the enormous potential for  
231 wood research in general and mycology in specific, though it should be remarked that  
232 although sub-micron resolution is obtained, resolution is lower even than conventional light  
233 microscopy. As illustrated by Trtik et al. (2007), scanning with a resolution below 1  $\mu\text{m}$   
234 results in a volume of the internal structure of wood (Fig. 1) down to details at cell wall level.  
235 These details are of importance when dealing with fungal growth in and decay of wood. It is  
236 common knowledge that fungi can penetrate very small openings. Bardage & Daniel (1997)  
237 tested the penetrative capacity of seven decay fungi. All of them were capable of penetrating

238 micropores of 0.6  $\mu\text{m}$  under certain experimental conditions but none of them could enter  
239 diameters smaller than 0.1  $\mu\text{m}$ . Therefore, anatomical structures such as pits, rays and axially  
240 oriented elements (Rayner & Boddy 1988) are important pathways of least resistance for  
241 fungal propagation in the wood, in addition to the bore holes created by hyphal tunnelling or  
242 cell wall degradation (Schwarze, 2007). Apparently, the mycelium can be discerned rather  
243 easily from the background noise when located outside the wood structure. A clear example is  
244 the picture of the fruiting bodies of *Aspergillus* and the tubular network of *Coriolus versicolor*  
245 (Fig. 2). The main difference between the two fungi is the pigmentation of the *Aspergillus*  
246 species. The melanin pigments, negatively charged and hydrophobic, confer a survival  
247 advantage to environmental microbes (Nosanchuk & Casadevall 2006) and to UV, solar and  
248 gamma radiation (Nosanchuk & Casadevall 2003). Moreover, some pigmented species exhibit  
249 a general attractive response to ionization (Zhdanova et al., 2004) or might even profit from  
250 radiation by using it as an energy source (Dadachova et al., 2007). This advantage also results  
251 in a better X-ray absorption and consequently a better visualization of melanin containing  
252 fungi. Other research of Van den Bulcke et al. (2008) already demonstrated the possible use  
253 of X-ray tomography for mycological research, more specifically by visualization of  
254 *Aureobasidium pullulans* on and in coated wood. This blue stain fungus was observable in the  
255 X-ray domain with a resolution down to 0.7  $\mu\text{m}$ . The difference with current research is  
256 twofold. First, the diameter of a blue stain fungus is on average larger (2-10  $\mu\text{m}$  and even up  
257 to 20  $\mu\text{m}$ ) than a white rot fungus (1.5-3.5  $\mu\text{m}$ ). Second, blue stain hyphae contain pigments.  
258 Therefore, it is expected that scanning of the smaller non-pigmented white rot fungi will be  
259 more difficult. For non-pigmented species the absence of strong X-ray absorbing component  
260 makes X-ray CT scanning difficult. Furthermore, while outside the wood, there is only  
261 interference from air, inside the substrate visualization and segmentation is more complicated,  
262 especially when dealing with the non-pigmented fungal species. Artefacts during scanning

263 and reconstruction can obscure their presence and that of interesting features. Scattering,  
264 fluorescence, polychromatic X-rays and noise are disturbing the ideal acquisition (Vidal et al.,  
265 2005). The phase contrast phenomenon can be another interfering factor, although it can be an  
266 advantage as well. While current tomography is absorption based, only recently the  
267 application of 3D phase contrast X-ray imaging is explored (Bronnikov, 2002; Groso et al.,  
268 2006; Trtik et al., 2007; Boone et al., 2009). For quantitative tomography, for instance when  
269 mapping density distributions, it is an artefact. But for qualitative tomography, it could help in  
270 visualizing biological tissue demonstrating weak absorption contrast. Possibly, further  
271 algorithmic filtering of the projections and of the reconstructed slices could also enhance  
272 image quality.

273 Comparison of the samples scanned before, after 1 week and after 6 weeks of exposure to the  
274 white rot fungus (Fig. 3) showed the formation of mycelial mats around the sample, yet with  
275 hyphae that were not fully connected. Segmentation of fungal tissue from wood and noise  
276 could clarify hyphal presence, yet interference with the phase contrast phenomenon decreased  
277 image quality in the interior of the wood substrate. Edges of wood had a similar grey level as  
278 fungi, which resulted in misclassification of some of the outer cell walls as fungal tissue.  
279 Furthermore, as the technique is based on density differences, it may not be possible to  
280 distinguish between degradation of the wood, fungal extracellular, fungal mucilage, fungal  
281 hyphae or other products/changes which also might lead to misclassifications. When  
282 examining the pine sapwood sample, penetration of hyphae seems to stop deeper than 40  $\mu\text{m}$   
283 in longitudinal direction beneath the surface. A plausible explanation is a combination of  
284 several effects, which resulted in a low growth of fungi and even complete arrest of growth.  
285 At first, contrary to pigmented species where a low radiation dose can be beneficial, for non-  
286 pigmented ones ionizing radiation imposes stress. During scanning this could have had an  
287 adverse effect, resulting in inactivation or even sterilization, which is only partly true

288 (radiation damage is a statistical process) as the dose at exposure only amounted up to 20 Gy,  
289 which is certainly not enough to eradicate all fungal growth (Uber & Goddard, 1934; Saleh et  
290 al., 1988; Dadachova et al., 2007). It should be remarked that radiation dose measurements  
291 with radiochromic fluids are not mimicking exposure conditions for the fungal tissue exactly,  
292 but the measured dose is far beneath the lethal doses mentioned in literature. Secondly, in  
293 order to obtain a high quality scan, the object of interest should sustain a stable position,  
294 which was a difficult task for the samples that were taken from the Petri-dish. Therefore,  
295 these samples needed some time to stabilize, causing dehydration. Third, small samples with  
296 even smaller objects of interest require scanning at very high magnification to achieve the  
297 sub-micron resolution. This implies that the samples must be located close to the warm X-ray  
298 tube during a sufficient long scantime due to the low flux. As such, a combination of radiation  
299 damage and dehydration / high temperature might have caused a growth stop. Therefore, old  
300 immobilized mycelial tissue might have blocked the pathways for the new hyphae, which  
301 could barely reach the wood axially, but could easily grow on the surface of the substrate.  
302 This is true for wood species with small wood cells, but for movingui and afzelia this effect is  
303 counteracted partly as pathways of penetration such as large vessels (Fig. 4) are not easily  
304 obstructed.

305 In order to discern fungal tissue from its surroundings objectively, the subtraction of a volume  
306 before and after exposure should result, in ideal circumstances, in the segmentation of fungal  
307 tissue and decayed wood parts, but the feasibility of doing so is limited for several reasons.  
308 First, as volumes are scanned on different times, registration is obligatory. The size of the  
309 volumes makes such a mathematical operation rather impracticable. Although rigid-body  
310 registration (Rajapakse et al., 2008) might be an option when compressed volumes are used  
311 (downscaled resolution and grey levels), this is problematic when dealing with wood and  
312 fungus. The wood substrate and the fungus as well represent a non-rigid structure that

313 manifests swell and shrink behaviour. Non-rigid registration (Crum et al., 2004) with free  
314 form transformation is necessary. Apparently, results (Fig. 5) are highly dependent on the  
315 quality of the scans and therefore insufficient for quantitative processing. This was expected  
316 as samples were scanned before incubation, put back and scanned again after fungal  
317 degradation and thus it was nearly impossible to retain the same position for every scan. As  
318 such, the orientation of the two volumes was quite different which complicated the problem,  
319 especially when dealing with an anisotropic substrate as wood. Pre-alignment was necessary  
320 in the first place. Secondly, resolution of two scans was not exactly the same and fungal  
321 degradation of the samples altered the structure substantially, making deformation registration  
322 a difficult task. An ideal set-up would fix the exposed sample in a sample-holder in the X-ray  
323 scanner and several scans should be performed without removal. However, if not workable  
324 the sample will be moved away from the X-ray scanner, which makes marking of the first  
325 position for rough re-placement of subsequent scans obligatory. Further fine-alignment could  
326 then be done as described in Viot et al. (2007). In fact, to overcome problems of dehydration,  
327 radiation induced stress, registration errors, etc the sample should be fixed in a miniaturized  
328 climate chamber.

329 Eventually, as form and function of decay fungi are difficult to study due to their action on  
330 different spatial and temporal scales and the complexity of the substrate, mathematical  
331 modelling could be a powerful complementary tool to amass knowledge concerning their  
332 growth and decay on solid wood, wood-based materials and re-engineered materials. In silico  
333 growth and decay on X-ray scanned volumes offers the possibility to compare with lab-  
334 degraded specimen. Theories of attack by white rot and by extension of brown rot, can be put  
335 to the test once a realistic set of parameters and environmental conditions concert the growth  
336 of the intercommunicating tubular network. In fact, any substrate could be subjected to fungal  
337 attack.

338

## 339 **5. Conclusions**

340

341 The mycelium of filamentous fungi consists of a network of tubular hyphae. Some of them  
342 are able to degrade wood and can cause substantial losses in the building industry. However,  
343 these fungi also play an important role in nutrient recycling and are applied in several  
344 industrial processes. In order to investigate their colonization strategies, research makes use of  
345 various imaging tools, of which sub-micron X-ray computed tomography is presented in this  
346 paper. Seemingly, pigmented fungal species are rather easy to visualize when growing outside  
347 the wood. The small hyphae of the most important non-pigmented wood decay fungi are more  
348 difficult to visualize due to their weak absorption and small size. Within the wood substrate,  
349 the combined effect of noise, artefacts and weak absorption obscures their presence even  
350 more. Manual segmentation based on the grey level histogram gave a clear view on the  
351 hyphal mass, but misclassifications occurred because of reconstruction artefacts. Apparently,  
352 growth was arrested due to radiation, dehydration and heat stress, blocking smaller anatomical  
353 structures. Further analysis of the samples with differential imaging was very complex.  
354 Changes to the set-up such as sterile working scan conditions, pre-fixation of the samples and  
355 alignment before scanning will considerably improve scan quality and increase the chances of  
356 success of differential imaging. Although automatic segmentation and quantification of fungal  
357 colonization was not possible in this stage of research, the hyphal mass was pictured using X-  
358 rays even in spite of noise interference. Future research will focus on pretreatment of the  
359 samples and fine tuning of the experimental set-up, hopefully leading to a contrast  
360 enhancement, better resolution and visualization of separate hyphae within the mycelium.  
361 Preferably, low doses and phase-contrast imaging could also contribute to superior scans.  
362 Ultimately, by combining non-destructive scanning and modelling of fungal growth with

363 realistic morphological and physiological characteristics, a powerful tool can be developed for  
364 predicting the influence of substrate and environmental conditions on growth and vice-versa  
365 in complex substrata such as wood.

366

367



368 **Acknowledgements**

369

370 The authors wish to thank the Fund for Scientific Research-Flanders (Belgium - FWO) for the  
371 postdoctoral funding granted to the first author.

372

373

374 **References**

375

376 ABU ALI, R., MURPHY, R.J. & DICKINSON, D.J. (1999). Investigation of the extracellular  
377 mucilaginous materials produced by some wood decay fungi. *Mycol Res* **103**, 1453-1461.

378

379 BARDAGE, S.L. & DANIEL, G. (1997). The ability of fungi to penetrate micropores:  
380 implications for wood surface coatings. *Mater Org* **31**, 233-245.

381

382 BECKETT, A. & READ, N. (1986). Low temperature scanning electron microscopy. In  
383 *Ultrastructural Techniques for Microorganisms*, Aldrich, H.C. & Todd, W.F. (Eds), pp. 45-  
384 86. New York: Plenum Press.

385

386 BOONE, M., DE WITTE, Y., DIERICK, M., VAN DEN BULCKE, J., VLASSENBOECK, J. & VAN  
387 HOOREBEKE, L. (2009). Practical use of the Modified Bronnikov Algorithm in micro-CT. *Nucl*  
388 *Instrum Methods Phys Res Sect B: Beam Interact Mater At* **accepted**.

389

390 BRONNIKOV, A.V. (2002). Theory of quantitative phase-contrast computed tomography. *J Opt*  
391 *Soc Am A - Opt Imag Sci Vis* **19**, 472-480.

392

393 CRUM, W.R., HARTKENS, T. & HILL, D.L.G. (2004). Non-rigid image registration: theory and  
394 practice. *Br J Radiol* **77**, S140-S153.

395

396 DADACHOVA, E., BRYAN, R.A., HUANG, X., MOADEL, T., SCHWEITZER, A.D., AISEN, P.,  
397 NOSANCHUK, J.D. & CASADEVALL, A. (2007). Ionizing Radiation Changes the Electronic  
398 Properties of Melanin and Enhances the Growth of Melanized Fungi. *PLoSone* **2**, e457.

399

400 DANIEL, G., VOLC, J. & NIKU-PAAVOLA, M.L. (2004). Cryo-FE-SEM & TEM immuno-  
401 techniques reveal new details for understanding white-rot decay of lignocellulose. *C R Biol*  
402 **327**, 861-871.

403

404 DICKSON, S. & KOLESIK, P. (1999). Visualisation of mycorrhizal fungal structures and  
405 quantification of their surface area and volume using laser scanning confocal microscopy.  
406 *Mycorrhiza* **9**, 205-213.

407

408 ERIKSSON, K.-E., BLANCHETTE, R.A. & ANDER, P. (1990). *Microbial and enzymatic*  
409 *degradation of wood and wood components*. Berlin: Springer-Verlag.

410

411 FALCONER, R.E., BOWN, J.L., WHITE, N.A. & CRAWFORD, J.W. (2005). Biomass recycling and  
412 the origin of phenotype in fungal mycelia. *Proc R Soc Lond Ser B - Biol Sci* **272**, 1727-1734.

413

414 GLOCKER, B., KOMODAKIS, N., PARAGIOS, N., TZIRITAS, G. & NAVAB, N. (2007). Inter and  
415 intra-modal deformable registration: Continuous deformations meet efficient optimal linear  
416 programming. In *20th International Conference on Information Processing in Medical*  
417 *Imaging*, Karssemeijer, N.L.B. (Ed.), pp. 408-420. Berlin: Springer-Verlag.

418

419 GREEN, F. & HIGHLEY, T.L. (1997). Mechanism of brown-rot decay: Paradigm or paradox. *Int*  
420 *Biodeterior Biodegrad* **39**, 113-124.

421

422 GROSO, A., ABELA, R. & STAMPANONI, M. (2006). Implementation of a fast method for high  
423 resolution phase contrast tomography. *Opt Express* **14**, 8103-8110.

424

425 GUTIERREZ, A., MARTINEZ, M.J., ALMENDROS, G., GONZALEZVILA, F.J. & MARTINEZ, A.T.  
426 (1995). Hyphal-sheath polysaccharides in fungal deterioration. *Sci Total Environ* **167**, 315-  
427 328.

428

429 HICKEY, P.C., SWIFT, S.R., ROCA, M.G. & READ, N.D. (2005). Live-cell imaging of  
430 filamentous fungi using vital fluorescent dyes. *Methods Microbiol* **34**, 63-87.

431

432 ILLMAN, B.L. & DOWD, B.A. (1999). High-resolution microtomography for density and  
433 spatial information about wood structures. In: *Proceedings of SPIE on Developments in X-*  
434 *ray Tomography II*, Bonse, U. (Ed.), pp. 198-204. Washington: Society of Photo-Optical  
435 Instrumentation Engineers.

436

437 KOMODAKIS, N., TZIRITAS, G. & PARAGIOS, N. (2007). Fast, approximately optimal solutions  
438 for single and dynamic MRFs. In *IEEE Conference on Computer Vision and Pattern*  
439 *Recognition*, pp. 960-967. Minneapolis: IEEE.

440

441 LIMAYE, A. (2006). *Drishti - Volume Exploration and Presentation Tool*. Baltimore: Vis.

442

443 MACCHIONI, N., PALANTI, S. & ROZENBERG, P. (2007). Measurements of fungal wood decay  
444 on Scots pine and beech by means of X-ray microdensitometry. *Wood Sci Technol* **41**, 417-  
445 426.

446

447 MANSUR, M., ARIAS, M.E., FLARDH, M. & GONZALEZ, A.E. (2003). The white-rot fungus  
448 *Pleurotus ostreatus* secretes laccase isozymes with different substrate specificities. *Mycologia*  
449 **95**, 1013-1020.

450

451 MASSCHAELE, B.C., CNUUDE, V., DIERICK, M., JACOBS, P., VAN HOOREBEKE, L. &  
452 VLASSEN BROECK, J. (2007). UGCT: new X-ray radiography and tomography facility. *Nucl*  
453 *Instrum Methods Phys Res Sect A: Accel Spectrom Detect Assoc Equip* **580**, 266-269.

454

455 McMILLIN, C.W. (1977). SEM technique for displaying 3-dimensional structure of wood.  
456 *Wood Sci* **9**, 202-204.

457

458 MULLER, U., BAMMER, R., HALMSCHLAGER, E., STOLLBERGER, R. & WIMMER, R. (2001).  
459 Detection of fungal wood decay using magnetic resonance imaging. *Holz Roh Werkst* **59**,  
460 190-194.

461

462 MULLER, U., BAMMER, R. & TEISCHINGER, A. (2002). Detection of incipient fungal attack in  
463 wood using magnetic resonance parameter mapping. *Holzforsch* **56**, 529-534.

464

465 NICOLE, M., CHAMBERLAND, H., RIOUX, D., LECOURE, N., RIO, B., GEIGER, J.P. & OUELLETTE,  
466 G.B. (1993). A cytochemical study of extracellular sheaths associated with *Rigidoporus*  
467 lignosis during wood decay. *Appl Environ Microbiol* **59**, 2578-2588.

468

469 NOSANCHUK, J.D. & CASADEVALL, A. (2003). The contribution of melanin to microbial  
470 pathogenesis. *Cell Microbiol* **5**, 203-223.

471

472 NOSANCHUK, J.D. & CASADEVALL, A. (2006). Impact of melanin on microbial virulence and  
473 clinical resistance to antimicrobial compounds. *Antimicrob Agents Chemother* **50**, 3519-3528.  
474

475 RÅBERG, U., TERZIEV, N. & LAND, C.J. (2007). Early soft rot colonization of Scots sapwood  
476 pine in above-ground exposure. *Int Biodeterior Biodegrad* DOI:10.1016/j.ibiod.2007.10.005.  
477

478 RAJAPAKSE, C.S., MAGLAND, J., WEHRLI, S.L., ZHANG, X.H., LIU, X.S., GUO, X.E. & WEHRLI,  
479 F.W. (2008). Efficient 3D rigid-body registration of micro-MR and micro-CT trabecular bone  
480 images. In: *Medical Imaging 2008 Conference*, REINHARDT, J.M.P.J.P.W. (Ed), pp. Z9142-  
481 Z9142. San Diego, CA: International Society of Optical Engineering.  
482

483 RAYNER, A.D.M. & BODDY, L. (1988). Fungal decomposition of wood - its biology and  
484 ecology. New York: John Wiley & Sons Ltd.  
485

486 REFSHAUGE, S., WATT, M., MCCULLY, M.E. & HUANG, C.X. (2006). Frozen in time: a new  
487 method using cryo-scanning electron microscopy to visualize root-fungal interactions. *New*  
488 *Phytol* **172**, 369-374.  
489

490 SALEH, Y.G., MAYO, M.S. & AHEARN, D.G. (1988). Resistance of some common fungi to  
491 gamma irradiation. *Appl Environl Microbiol* **54**, 2134-2135.  
492

493 SCHWARZE, F. (2007). Wood decay under the microscope. *Fungal Biol Rev* **21**, 133-170.  
494

495 TRTIK, P., DUAL, J., KEUNECKE, D., MANNES, D., NIEMZ, P., STAHLI, P., KAESTNER, A.,  
496 GROSO, A. & STAMPANONI, M. (2007). 3D imaging of microstructure of spruce wood. *J Struct*  
497 *Biol* **159**, 46-55.

498

499 UBER, F.M. & GODDARD, D.R. (1934). Influence of death criteria on the X- ray survival  
500 curves of the fungus, *Neurospora*. *J Gen Physiol* **17**, 577-590.

501

502 VAN DEN BULCKE, J., MASSCHAELE, B., DIERICK, M., VAN ACKER, J., STEVENS, M. & VAN  
503 HOOREBEKE, L. (2008). Three-dimensional imaging and analysis of infested coated wood with  
504 X-ray submicron CT. *Int Biodeterior Biodegrad* **61**, 278-286.

505

506 VIDAL, F.P., LETANG, J.M., PEIX, G. & CLOETENS, P. (2005). Investigation of artefact sources  
507 in synchrotron microtomography via virtual X-ray imaging. *Nucl Instrum Methods Phys Res*  
508 *Sect B: Beam Interact Mater At* **234**, 333-348.

509

510 VIOT, P., BERNARD, D. & PLOUGONVEN, E. (2007). Polymeric foam deformation under  
511 dynamic loading by the use of the microtomographic technique. *J Mater Sci* **42**, 7202-7213.

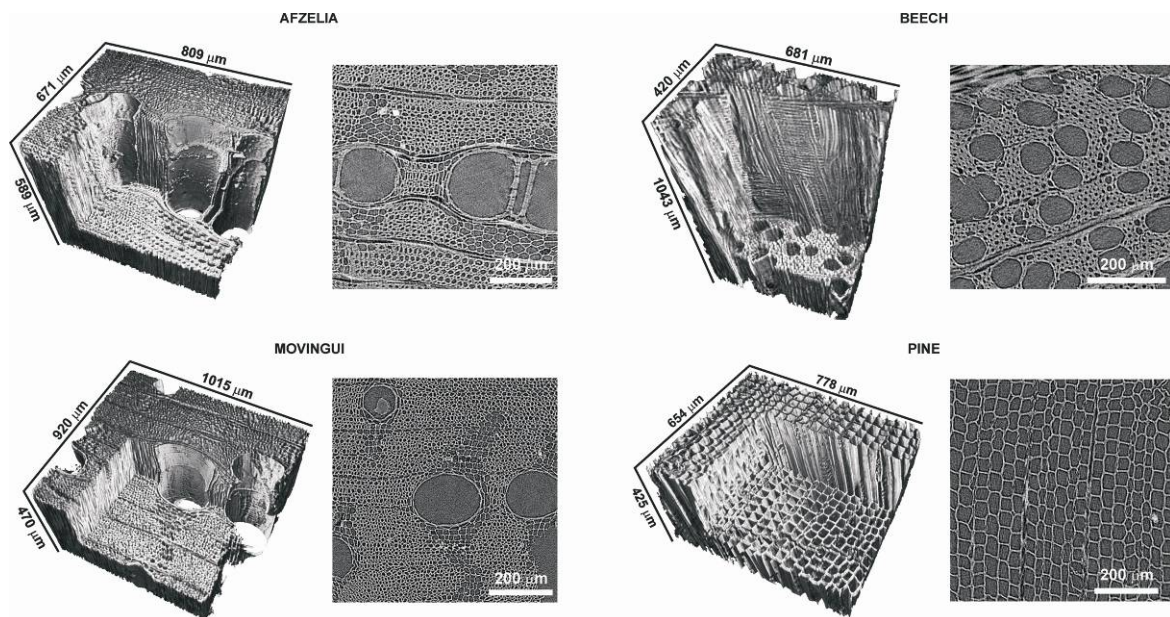
512

513 VLASSENBROECK, J., DIERICK, M., MASSCHAELE, B., CNUDE, V., VAN HOOREBEKE, L. &  
514 JACOBS, P. (2007). Software tools for quantification of X-ray microtomography at the UGCT.  
515 *Nucl Instrum Methods Phys Res Sect A: Accel Spectrom Detect Assoc Equip* **580**, 442-445.

516

517 ZHDANOVA, N.N., TUGAY, T., DIGHTON, J., ZHELTONOZHISKY, V. & MCDERMOTT, P. (2004).  
518 Ionizing radiation attracts soil fungi. *Mycol Res* **108**, 1089-1096.

519



520

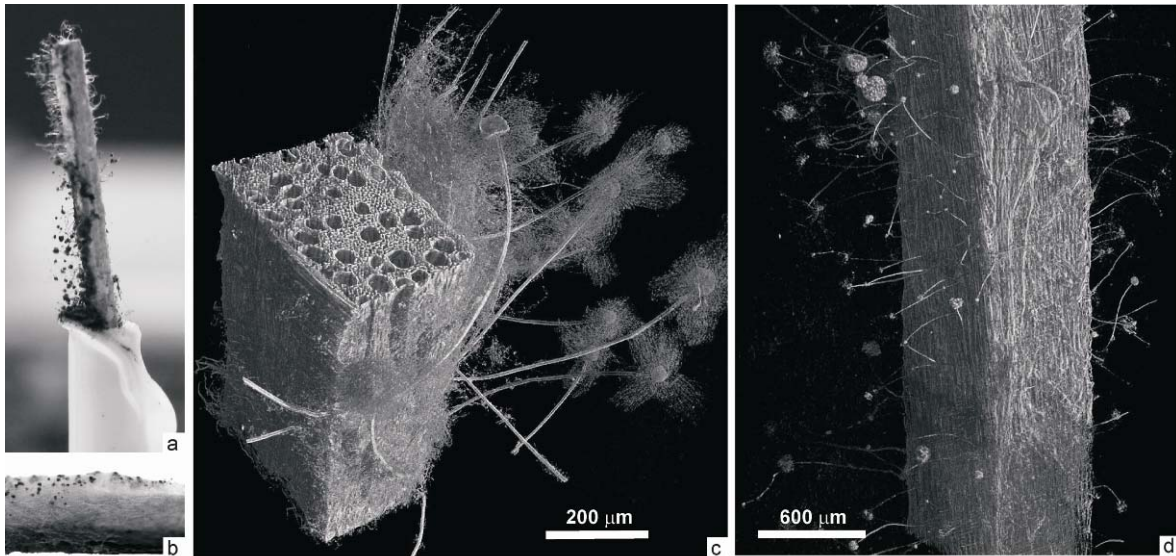
521

522 **Figure 1.** Three-dimensional reconstructions of the tested wood samples before exposure to  
523 the fungal culture of *Coriolus versicolor* and a cross-sectional view as an illustration of the  
524 level of detail.

525

526





527

528

529 **Figure 2.** Images in the visible wavelength domain of beech (a) and pine (b) covered with

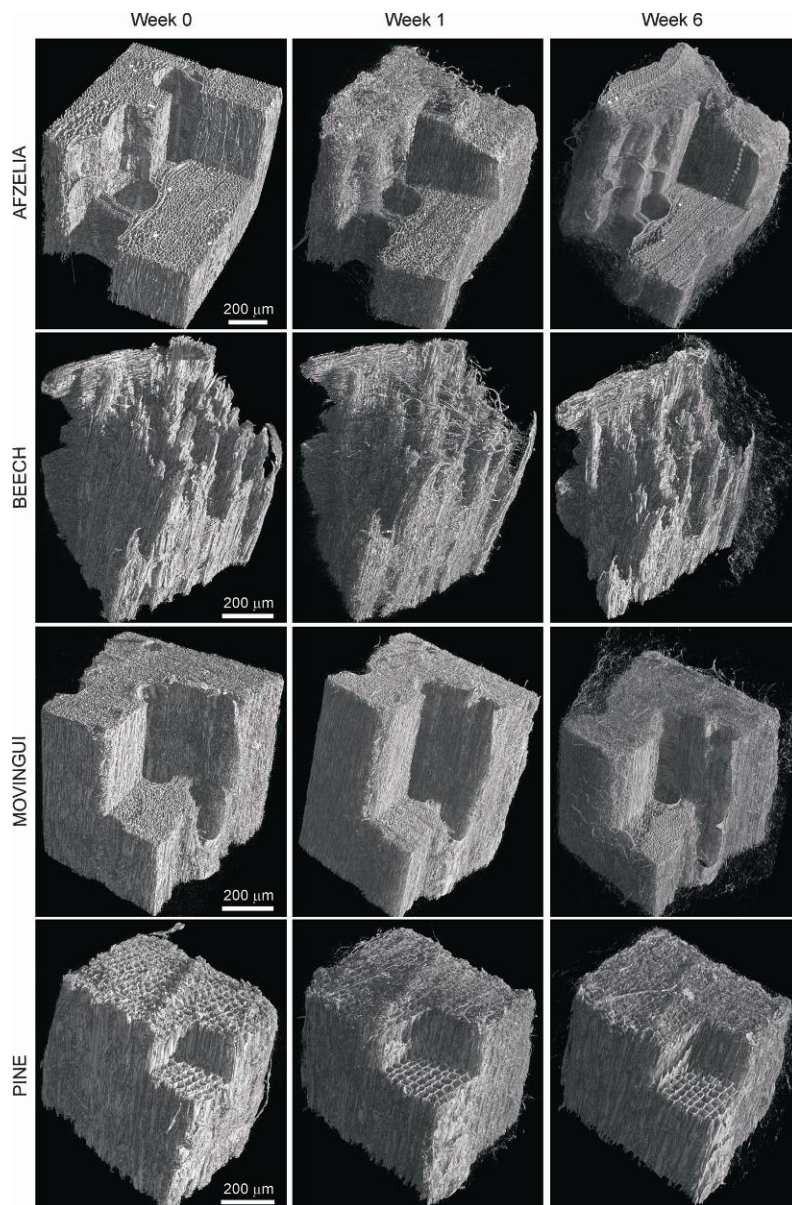
530 *Coriolus versicolor*, *Aspergillus* and other unidentified moulds. Reconstructions of X-ray

531 scans for beech (c) and pine (d) showing *Aspergillus* and a view on the internal structure of

532 beech.

533

534



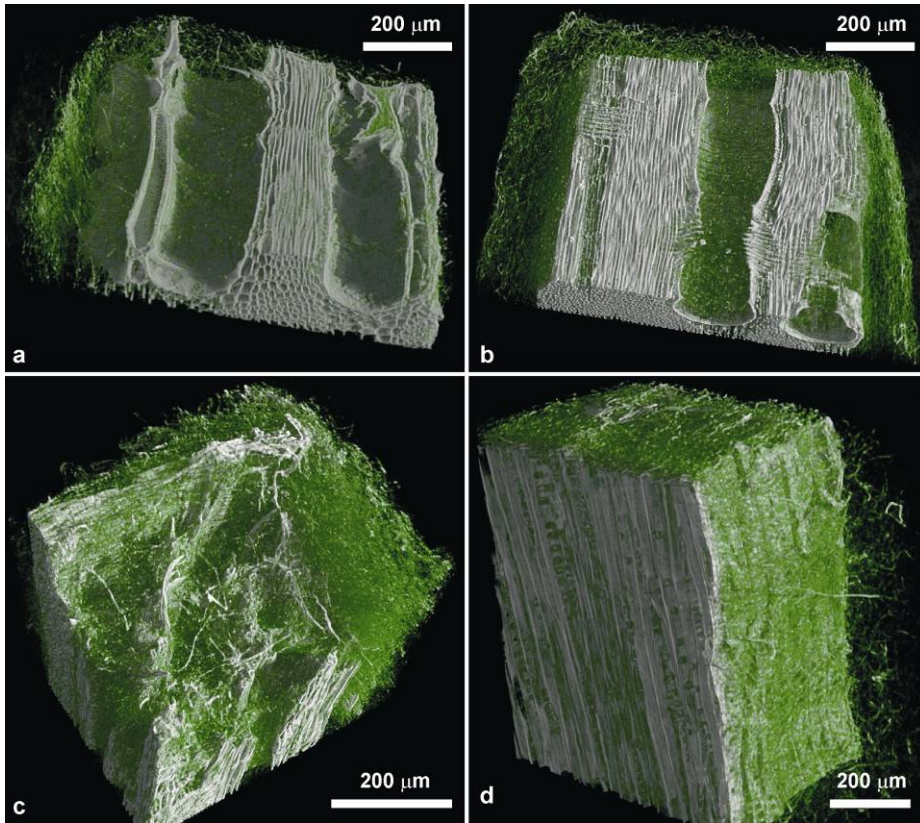
535

536

537 **Figure 3.** Time series scanning of the 4 wood samples under study: reconstruction before  
 538 exposure to the fungi and after 1 and 6 weeks of incubation.

539

540



541

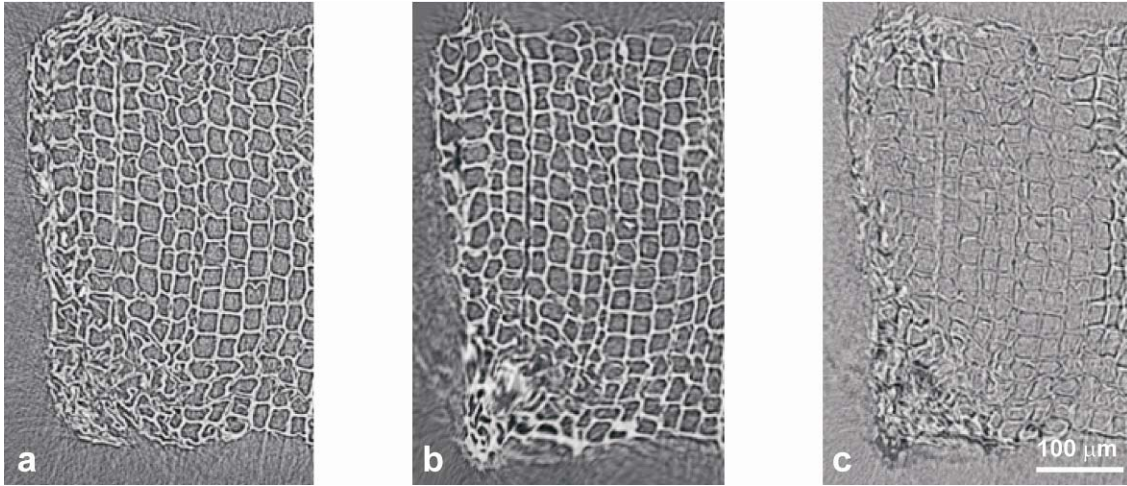
542

543 **Figure 4.** Segmentation of hyphae (green) on the afzelia (a), movingui (b), beech (c) and pine

544 (d) volumes.

545

546



547

548

549 **Figure 5.** Reconstructed slice before exposure (a), image of the same slice after 6 weeks of

550 exposure to the fungi and non-rigid transformation (b) and difference (c) between (a) and (b).

551